

This article was downloaded by:

On: 22 January 2011

Access details: *Access Details: Free Access*

Publisher *Taylor & Francis*

Informa Ltd Registered in England and Wales Registered Number: 1072954 Registered office: Mortimer House, 37-41 Mortimer Street, London W1T 3JH, UK



## The Journal of Adhesion

Publication details, including instructions for authors and subscription information:

<http://www.informaworld.com/smpp/title~content=t713453635>

### Interaction forces measured between mica-adsorbed quaternarized poly(2-vinylpyridine) layers: Effects of pH and compression

George Maurdev<sup>a</sup>; Laurence Meagher<sup>a</sup>; Michelle L. Gee<sup>a</sup>

<sup>a</sup> School of Chemistry, University of Melbourne, Victoria, Australia

Online publication date: 08 September 2010

**To cite this Article** Maurdev, George , Meagher, Laurence and Gee, Michelle L.(2003) 'Interaction forces measured between mica-adsorbed quaternarized poly(2-vinylpyridine) layers: Effects of pH and compression', *The Journal of Adhesion*, 79: 10, 937 – 953

**To link to this Article:** DOI: 10.1080/714906146

**URL:** <http://dx.doi.org/10.1080/714906146>

PLEASE SCROLL DOWN FOR ARTICLE

Full terms and conditions of use: <http://www.informaworld.com/terms-and-conditions-of-access.pdf>

This article may be used for research, teaching and private study purposes. Any substantial or systematic reproduction, re-distribution, re-selling, loan or sub-licensing, systematic supply or distribution in any form to anyone is expressly forbidden.

The publisher does not give any warranty express or implied or make any representation that the contents will be complete or accurate or up to date. The accuracy of any instructions, formulae and drug doses should be independently verified with primary sources. The publisher shall not be liable for any loss, actions, claims, proceedings, demand or costs or damages whatsoever or howsoever caused arising directly or indirectly in connection with or arising out of the use of this material.

## INTERACTION FORCES MEASURED BETWEEN MICA-ADSORBED QUATERNARIZED POLY(2-VINYLPYRIDINE) LAYERS: EFFECTS OF pH AND COMPRESSION

**George Maurdev**  
**Laurence Meagher**  
**Michelle L. Gee**

School of Chemistry, University of Melbourne, Victoria, Australia

*The surface forces apparatus was used to measure directly the interaction forces between mica-adsorbed quaternarized poly(2-vinylpyridine) (QP2VP) layers as a function of solution pH. The interaction is repulsive at large-surface separations and is dominated by a double layer interaction. At shorter range, electrosteric forces dominate until, at small-surface separations, attractive bridging forces lead to intersurface adhesion. The bridging attractive forces are attributed to both intersurface bridging and polyelectrolyte chain entanglement. These are extremely sensitive to the conformation of the adsorbed polyelectrolyte, which changes significantly with solution pH.*

*Surface forces measured on compression of the adsorbed QP2VP layers do not clearly reflect changes in the adsorbed conformation and surface excess of this polyelectrolyte. Rather, the polyelectrolyte conformation is manifest more dramatically on measurement of adhesion, upon retraction/decompression of the surfaces from contact. There is a strong dependence of the adhesion between the polyelectrolyte layers on the compressive load, time in contact, and compression history since the molecular rearrangements required for chain entanglement and intersurface bridging occur on a long time scale, i.e., of the order of minutes. Under a small*

Received 23 February 2003; in final form 9 July 2003.

One of a Collection of papers honoring Jacob Israelachvili, the recipient in February 2003 of *The Adhesion Society Award for Excellence in Adhesion Science, Sponsored by 3M*.

The authors, particularly Michelle L. Gee, thank the Australian Research Council for their generous support of this work in the form of an ARC Large Grant. We also thank Professor Tom Healy for his support during the developmental stages of this project.

Current address of George Maurdev is CSIRO, Textile and Fibre Technology, P.O. Box 21, Belmont, Victoria, 3216, Australia.

Current address of Laurence Meagher is CSIRO, Molecular Science, Bag 10, Clayton South, Victoria 3169, Australia.

Address correspondence to Michelle L. Gee, School of Chemistry, University of Melbourne, Victoria, 3010, Australia. E-mail: mlgee@unimelb.edu.au

| compressive load, the surfaces are closer together, facilitating segment-surface and segment-segment interactions across the two interacting layers.

## INTRODUCTION

Increasing our understanding of the mechanisms by which polyelectrolytes modify colloidal interactions is crucial to a vast array of areas, from processes within the mining industry to paint manufacturing and waste water treatment, to name just a few. It is for this reason that surface forces between adsorbed polyelectrolyte layers have been the focus of much study, both experimental [1–4] and theoretical [5–9]. Previous workers have investigated how polyelectrolytes influence colloidal interactions by direct force measurements, monitoring the effects on surface forces of polyelectrolyte concentration [10, 11], molecular weight [1], charge density [12], solution pH [2, 13], background salt concentration [4], and polyelectrolyte adsorption history [14, 15]. Maurdev [16] and Fler *et al.* [17] contain general reviews of this literature.

As part of a series of work by us, we used the surface forces apparatus to study how the interactions between two mica surfaces are modified by the adsorption of quaternarized poly(2-vinylpyridine) (QP2VP) [18]. We related the measured surface forces to the adsorbed conformation of this polyelectrolyte, which we determined spectroscopically [19]. It was found that the surface excess and adsorbed conformation of QP2VP, which are dependent on solution pH, influence the nature of the surface interactions. The layers become more compact with increasing pH, inhibiting polymer chain interpenetration across the two surfaces, thus limiting adhesion [19].

This article constitutes the third article in the series in which we investigate how the adsorption of QP2VP affects colloidal interactions. Specifically, we use the surface forces apparatus to investigate how the adsorption history of QP2VP affects colloidal interactions. To this end, we adopt an experimental protocol in which we measure the surface forces between mica-adsorbed QP2VP layers as a function of solution pH, as was done in Maurdev *et al.* [18]. However, initial adsorption is at a high pH, and subsequent surface forces are measured as pH is decreased. To highlight any history dependence, we compare our present results with those in Maurdev *et al.* [18], where initial adsorption was at a low pH. We also investigate how the surface forces and adhesion (bridging) vary with time in contact and compressive load, allowing us to monitor how compression of the QP2VP

layers affects rearrangement of and interpenetration between the polyelectrolyte chains.

## EXPERIMENTAL SECTION

### Materials

Ruby muscovite mica was obtained from S & J Trading (New York, USA) and was cleaved in order to obtain several molecularly smooth single crystals  $1\text{ cm}^2$  in area and  $\sim 1\text{--}2\ \mu\text{m}$  thick.

Water used in all solutions was obtained from a Milli-Q Plus™ water purification system, which was fed by a reverse osmosis water purification system. The final pure water obtained had a resistivity of  $18.2\ \text{M}\Omega\text{cm}$ . All chemicals used for preparing solutions or cleaning were of AR grade. Sodium iodide (ICN Biomedicals Inc. Aurora, Ohio, USA), hydriodic acid (Merck Pty. Ltd.) and both nitric acid and sodium hydroxide (APC Seven Hills, NSW, Australia) were used as received. RBS 35 Detergent, was supplied by PIERCE (Illinois, USA). AR grade ethanol (APC Seven Hills, NSW, Australia) was redistilled from an all-Pyrex still. Nitrogen gas (BOC Gases) was passed through a hydrocarbon moisture trap and finally a  $0.45\ \mu\text{m}$  particle filter.

The polyelectrolyte used in this study was QP2VP and was a gift from Dr. Alain Hill of Bristol University. The repeating unit is illustrated in Figure 1. It is comprised of vinyl pyridine monomers, which are quaternarized by methyl iodide such that 76% of the repeating units bear a permanent positive charge, statistically distributed along the polyelectrolyte backbone. The remaining 24% of the monomer units are comprised of the ionisable vinyl pyridine groups. These groups have a  $\text{pK}_a$  of around 5.25, similar to that of pyridine [20], which we confirmed by a simple charge titration. The average number of repeat units on this polyelectrolyte is 170, corresponding to a molecular weight of  $36,000\ \text{g mol}^{-1}$ .

### Cleaning Procedures

All internal parts of the surface forces apparatus were sonicated in 1% RBS detergent solution for 1 h, soaked in 10% nitric acid overnight, and then soaked in ethanol overnight, with the exception of the magnet assembly, which was not treated with acid. All parts were rinsed with copious amounts of Milli-Q water between each soaking. Prior to assembly, each part was rinsed with redistilled ethanol and blown dry with purified nitrogen gas. Glassware was cleaned by soaking in

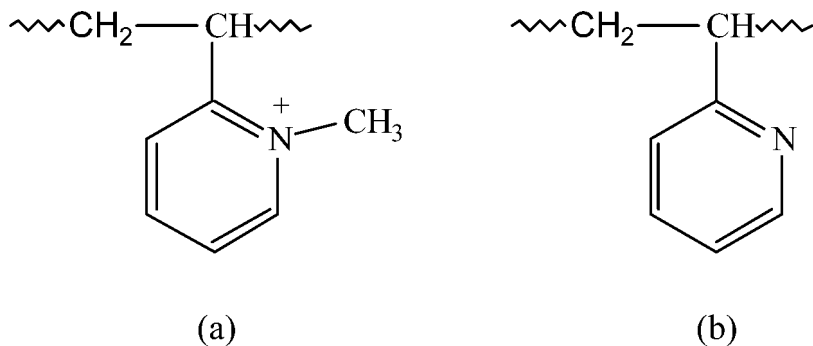


**FIGURE 1** Structure of the repeat units of quaternarized poly(2-vinylpyridine): (a) quaternarized residues comprising 76% of the total chain, and (b) nonquaternarized residues comprising 24% of the residues containing iodide counter-ions. (a) and (b) are arranged in a statistical distribution along the polyelectrolyte backbone.

a 10% w/w aqueous NaOH solution for 30 min and then rinsed with copious amounts of Milli-Q water just prior to use.

## Apparatus

All measurements obtained in this study were made using a modified surface forces apparatus (SFA) [18]. The principles behind the SFA for measurement of colloidal interactions have been well described elsewhere [21]. Briefly, two thin sheets of mica are back-silvered to a transmittance of  $\sim 5\%$ , and each sheet is glued to a hemicylindrical silica disc. The disks are then mounted in a crossed cylinder conformation in the apparatus. Surface separation is measured using a FECO (fringes of equal chromatographic order) interference pattern, which allows measurement of the surface separation with an accuracy of  $\sim \pm 0.1$  nm [21–23]. Zero surface separation is defined as mica-mica contact, and all intersurface separations quoted here are relative to this. The top surface is rigidly mounted, whereas the lower surface is mounted on a double cantilever spring of known force constant. The separation between the surfaces is controlled by a series of motors described below. Interaction between the surfaces is manifest as a deflection of the spring to which the bottom surface is attached. Hence, using Hooke's Law, the measured spring deflection yields the force of interaction between the two surfaces.

Typically, in the SFA mechanical motors allow coarse adjustment of surface separation, and fine adjustment is achieved *via* a piezo-electric

crystal. In our modified SFA, a magnetic force transducer (MFT) is employed instead of the piezo-electric crystal. The operation of the magnetic force transducer entails the attachment of a magnet to the lower surface and a magnetic transducer fastened to the underside of the SFA [24]. A variable magnetic field, produced by applying a voltage across the transducer, exerts a force on the magnet attached to the lower surface, thus allowing the accurate adjustment of surface separation over a range of 0 to 5  $\mu\text{m}$ . The sensitivity obtained is equivalent to that of a piezo-electric crystal, *i.e.*, subnanometer sensitivity in movement. Advantages of the MFT over the piezo-electric crystal are that its response is very linear, nonhysteretic and less prone to drift through thermal conduction.

During force measurements, surface separation was adjusted very slowly to allow time for molecular rearrangement of adsorbed QP2VP and to minimise velocity-dependent effects on the force curves, thus yielding a force curve as close to equilibrium as possible. All forces measured were scaled by the geometric mean of the radii of curvature of the contact zone by placing a dovetail prism in the path of the transmitted light [24]. According to the Derjaguin approximation [23], the resulting scaled force between two crossed cylinders is equivalent to the interaction between a sphere and a flat surface. Scaling the force in this manner allows us to compare force profiles from one experiment to another.

## Experimental Protocol

Interaction forces were measured between physisorbed polyelectrolyte layers that were formed by allowing QP2VP to adsorb onto bare mica surfaces from a stock solution containing 100 ppm QP2VP, with a background electrolyte of  $1 \times 10^{-4}$  M NaI at pH 7.5. The surfaces were equilibrated with the polyelectrolyte solution for a minimum of 4 h before measurements were taken to allow sufficient time for adsorption of the polyelectrolyte. Further adjustments in pH were made by draining the SFA cell but leaving a droplet of solution between the mica surfaces and then filling the cell with new stock solution adjusted to the required pH. All pH adjustments were made using solutions of hydriodic acid and sodium hydroxide.

## RESULTS AND DISCUSSION

Note that all force profiles are presented as semilog plots where the scaled force,  $F/R$ , is on a logarithmic scale and surface separation is plotted linearly. This aids visual identification of electrical double

layer forces, which decay exponentially with surface separation and so appear linear on such a plot.

### Effects of pH on Surface Interactions

The forces measured between mica surfaces with adsorbed QP2VP at each of the three pH conditions, 7.5, 6.3, and 4.1, are shown in Figure 2. Note that forces are monotonically repulsive at each pH. This is indicative of a long-range electrical double layer interaction. Therefore, we used the DLVO [23, 26] theory to predict the force

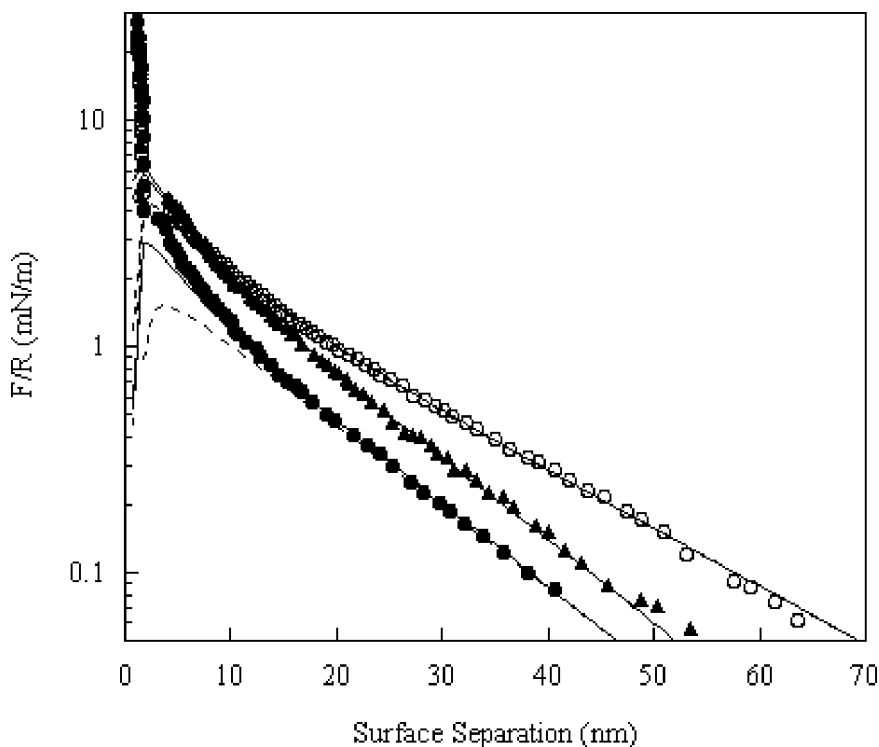


**FIGURE 2** Semilog plots of normalised force versus surface separation between mica surfaces with adsorbed QP2VP at pH 7.5 (●), pH 6.3 (○), and pH 3.9 (▲). The solid curves represent the DLVO theoretical fit to the experimental data. The upper and lower limits are the constant charge and constant potential boundary conditions, respectively. The best fits were obtained using a Hamaker constant of  $2.2 \times 10^{-20}$  J. The surface potentials, Debye lengths, and hard wall positions are presented in Table 1.

profile for two mica surfaces interacting across water. This was calculated using the nonlinear Poisson-Boltzmann equation for the double layer interaction *via* the algorithm developed by McCormack *et al.* [27]. We used a Hamaker constant of  $2.2 \times 10^{-20}$  J [23] for the van der Waals contribution to the total interaction. The electrostatic surface potential and the Debye length were used as fitting parameters to the data. The DLVO predictions thus obtained also appear as solid lines in Figure 2 for comparison with the experimentally measured force profiles. The upper and lower curves for each fit correspond to constant surface charge and constant surface potential boundary conditions, respectively. Clearly, for each force profile, the repulsive interaction is well described by DLVO theory at surface separations greater than 15 nm, indicating that beyond this range of surface separations there is little or no extension of the adsorbed polyelectrolyte into solution, normal to the surface.

The surface potentials and Debye lengths resulting from the DLVO fits to the force profiles are given in Table 1. Note that the values of the Debye length are within experimental error of each other, as expected, since the background concentration of NaI is approximately the same at each pH. Any small variation in electrolyte concentration, and hence Debye length, is due to polyelectrolyte's counter-ions and added acid or alkali required to adjust pH.

The values of surface potential in Table 1 are quoted as positive since we established in earlier work that adsorption of QP2VP on mica, under the solution conditions used in this study, results in overcompensation of the surface charge, *i.e.*, charge at the interface is dominated by the positively charged polyelectrolyte [18]. As mentioned above, the surface potential was obtained by fitting the nonlinear Poisson-Boltzmann equation to the electrical double layer repulsion at long range. In order to accomplish a fit, the position of the Outer Helmholtz Plane (OHP) must be assumed, and here mica-mica contact was chosen. This is an approximation since the adsorbed polyelectrolyte layer is of a finite thickness and is itself a source of

**TABLE 1** Position of the Hard Wall Repulsion and Results of the DLVO Fit to the Measured Force Profiles (from Figures 2 and 3) for the Interaction Between Mica-Adsorbed QP2VP as a Function of pH

Solution pH	Surface potential (mV)	Debye length (nm)	Hard wall position (nm)
7.5	$80 \pm 5$	12	1.2
6.3	$120 \pm 5$	16	1.4
3.9	$115 \pm 5$	12	1.4



charge. However, we have ignored this here since the position of the hard wall repulsion varies by no more than 2 Å from experiment to experiment (see Table 1). Nonetheless, despite these approximations, the validity of which have been discussed elsewhere [18], we can gain insight by looking at trends in the fitted surface potentials. We do this in the following discussion.

Table 1 shows that, at pH 7.5, the DLVO fit to the force profile for the interaction between adsorbed QP2VP layers gives a surface potential,  $\psi_o$ , of 80 mV. A decrease in solution pH to 6.3 yields a fitted  $\psi_o$  of 120 mV. This increase in the net surface potential is a result of the increase in charge density of the QP2VP since more of the non-quaternarized pyridine groups along the polyelectrolyte chain (which have a  $pK_a$  of 5.25 [20]) become protonated as pH is reduced. Additionally, a drop in pH also results in a decrease in the negative charge on the underlying mica surface [28–30], which further contributes to an increase in the net positive surface potential and a corresponding increase in the range of the double layer repulsion (Figure 2). Interestingly, however, a further reduction in pH to 3.9 leads to a drop in the  $\psi_o$  to 115 mV, which suggests that some polyelectrolyte desorbs at this pH. This is an expected result since, in our earlier spectroscopic study on the adsorption of QP2VP on silica [19], we also measured a dependence of the surface excess on pH. See Table 2 for these data.

The same profiles presented in Figure 2 are presented again in Figure 3 on an expanded scale to highlight detail of the force profiles at small surface separations. At pH 7.5, the repulsive interaction deviates significantly from DLVO theory at intersurface spacings below 15 nm. This deviation is attributed to electrosteric repulsion [17] between the surfaces. That is to say, the adsorbed layers contain a significant proportion of charged polymer segments, looping and tailing into solution, and their counter-ions, the compression of which

**TABLE 2** Data on the Adsorption from Solution of QP2VP on Silica, as a Function of pH

pH	Surface excess ( $\text{mg m}^{-2}$ )	Centre of mass (nm)
2.6	0.24	28
4.5	0.48	20
6.6	0.82	16
8.1	1.16	10

Specifically, the surface excess and centre of mass of QP2VP were measured. The data was obtained by us using an evanescent wave spectroscopic method [19].

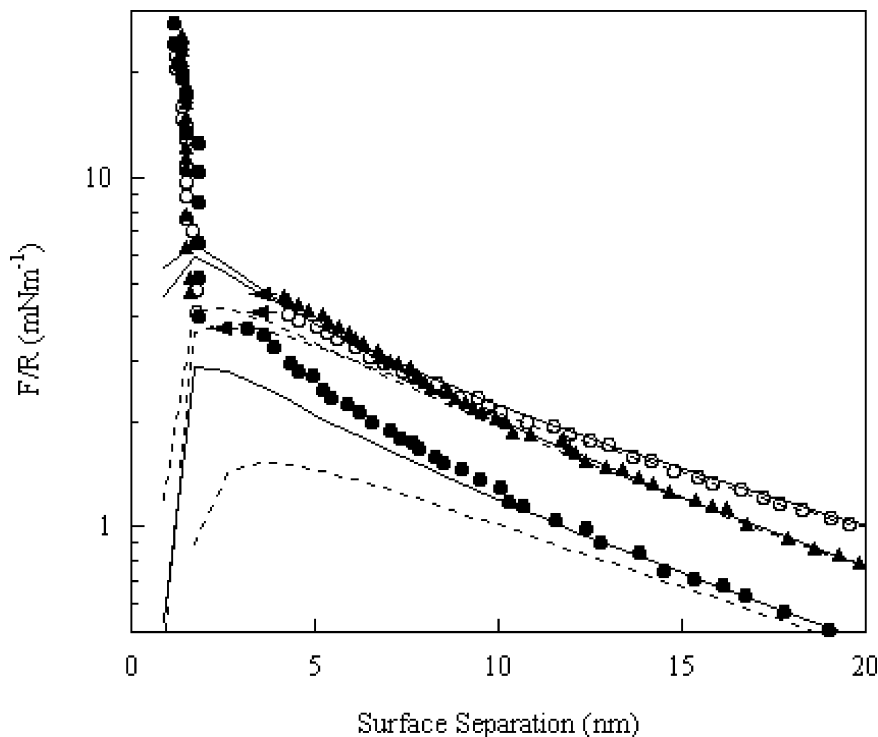


**FIGURE 3** Semilog plots of normalised force versus surface separation between mica surfaces with adsorbed QP2VP at pH 7.5 (●), pH 6.3 (○), and pH 3.9 (▲), as per Figure 2, but displayed on an expanded scale to highlight surface interactions at small separations. The arrows indicate the position of attractive jumps into contact.

gives rise to this additional repulsion. Typically, in the absence of adsorbed polyelectrolyte, the forces between bare mica surfaces at this ionic strength are well described by the DLVO theory with the magnitude of the repulsion intermediate between constant charge (upper solid line) and constant potential (lower solid line) boundary conditions. In contrast, the repulsive forces measured at pHs 4 and 6 are well described by DLVO theory down to surface separations as small as 4 nm. It is possible that the significant increase in the electrical double layer repulsion at each of these pHs obscures the electrosteric forces present at small intersurface spacings. It is nonetheless tempting to suggest that the proportion of polyelectrolyte loops and tails extending away from the surface is reduced at lower pH values, but this contradicts our spectroscopic evidence to the contrary

(Table 2) in which we measure an increase in the centre of mass of the adsorbed layer as pH is reduced.

As an aside, we have chosen not to subtract the predicted repulsive electrostatic and attractive van der Waals forces from the force profiles to elucidate the details of the electrosteric repulsion since we cannot accurately calculate the electrical double layer and van der Waals forces in this system at small surface separations. Note that, if the outer Helmholtz plane were moved to the hard wall (not shown here), a lower surface potential may be fitted: however, the quality of the fit and the trends observed do not alter the interpretation presented here.

### Interactions at Small Surface Separations

From Figure 3 it is clear that the surface forces measured under all pH conditions exhibit a strong attractive force manifest as an inward jump of the surfaces towards each other at surface separations of  $\sim 2\text{--}4$  nm. These inward jumps are marked on the force profile to which they correspond. The attractive force measured here is greater in magnitude than the expected van der Waals attraction and so is attributed to polymer bridging, as seen previously in this system [18]. The optimal conditions for polymer bridging are when the polyelectrolyte has a strong affinity for the oppositely charged surface to which it is adsorbed and adsorption occurs from a low ionic strength solution [3, 4, 10, 12]. These conditions are satisfied in our mica-adsorbed QP2VP system.

After the initial attractive jump into contact, the interaction becomes steeply repulsive with little or no change in surface separation, marking the position of the hard wall repulsion (Figure 3). This steep hard wall is indicative of little or no compressibility of the adsorbed QP2VP layers. On repeated compression, there is no significant change in the surface forces and the position of the hard wall does not change and is independent of pH, as indicated in Table 1. These observations are very different from those made in a similar study by Maurdev et al. in which QP2VP was initially adsorbed at low pH, rather than high pH [18]. In this previous work, increases in solution pH led to increased adsorption, shifting the position of the hard wall to larger surface separations. We also found in this earlier work that there is a distinct hysteresis between initial and subsequent compressions of the adsorbed QP2VP layer. This hysteresis is not observed in the results presented here, as mentioned above.

Clearly, the pH at which QP2VP is initially adsorbed affects the structure of the adsorbed layer found after subsequent changes in pH. QP2VP's affinity for a negatively charged surface such as mica

or silica increases with increasing pH leading to more points of contact between the polyelectrolyte and the surface and, hence, a reduction in the looping and tailing into solution, thus forming a more compact adsorbed layer [19] (see Table 2). Therefore, if initial adsorption is at a high pH, any subsequent change in pH does not alter the polyelectrolyte conformation to any significant extent, at least on the time scale of these experiments, since many points of attachment of the QP2VP to the mica must be broken to achieve this. Hence the force profiles show no hysteresis and the position of the hard wall does not change upon compression. On the other hand, if initial adsorption is at a low pH, the polyelectrolyte exhibits more looping and tailing into solution with fewer points of attachment to the surface. Therefore, the adsorbed layer is compressible and subsequent variations in pH result in changes in the conformation of the adsorbed QP2VP with greater efficacy.

### Effects pH on Intersurface Adhesion

After the adsorbed QP2VP layers are brought into contact with no positive loading, subsequent retraction of the surfaces results in a rapid adhesive jump out of contact, *i.e.*, a strong adhesive force is measured and the opposing force required to separate the surfaces is equal to the force of adhesion between them. The adhesion thus measured is  $4.5 \text{ mN m}^{-1}$  at pH 7.5. Note that the surfaces remain at their hard wall position until the jump out and that there is no flattening of the contact zone. The magnitude of the adhesive force is reproducible for successive retractions. When the solution pH is 3.9, the adhesion between the surfaces is  $\sim 20 \text{ mN.m}^{-1}$ . This coincides well with previous work, in which it was also found that the force of adhesion between QP2VP layers was maximised at low pH [18]. This is a sensible result in light of adsorbed polyelectrolyte conformation: at low pHs there is less adsorbed polyelectrolyte and there is more looping and tailing into solution (Table 2). Hence, there is more potential for chain entanglement and intersurface bridging, and so adhesion is stronger.

The situation is different at pH 6.3, where successive retractions of the contacted surfaces result in an increase in adhesion from  $2.5 \text{ mN.m}^{-1}$  to  $4.7 \text{ mN.m}^{-1}$ , then reaching a plateau at around  $7.2 \text{ mN.m}^{-1}$ . We have already established that, at pH 6.3, the attraction between QP2VP and a negatively charged surface is not as strong as occurs at higher values of pH. This is reflected in the measured surface excesses and centre of mass (see Table 2 and discussion above). Hence, repeated retraction of the contacted surfaces more readily perturbs the structure of the more loosely bound polyelectrolyte

layers, enhancing adhesion. We can, at best, only speculate about the exact detailed mechanism of this phenomenon, but one possibility is that, at pH 6.3, some of the QP2VP within the interfacial region is only weakly associated with the surface. Repeated adhesive contact between the two surfaces might force some segments of the loosely associated molecules to reattach to the surface, anchoring the polyelectrolyte more strongly at these points. It is also possible that repeated retraction “teases out” some polyelectrolyte chains. Hence, the more strongly anchored polyelectrolyte is more able to oppose retraction of the surfaces, and the increased looping and tailing facilitates chain entanglement. Both of these effects will tend to increase adhesion. Note that this would not happen at pH 3.9 since there is less affinity of QP2VP for the surface at this pH.

The change in adhesion as a function of pH (discussed above) irrefutably indicates a change in the adsorbed layer as a result of molecular rearrangements and limited desorption, as per Table 2. However, the position of the hard wall repulsion changes by no more than 2 Å throughout all the force measurements presented in Figure 3 (see Table 1). Claesson *et al.* [12] elegantly showed the effect that polyelectrolyte charge density has on the adsorbed conformation of polyelectrolytes, *i.e.*, with decreasing polyelectrolyte charge density the adsorbed conformation becomes more extended and the hard wall position increases. The authors use the position of the hard wall as an indicator of the adsorbed polyelectrolyte conformation. We believe that, in that case, this description was sufficient to present an argument to demonstrate the changes in the layers with changing polyelectrolyte linear charge density. However, caution must always be exercised and other corroborative data must be assessed to clearly describe changes in adsorbed macromolecular conformation from surface forces data, since the hard wall is affected by the compressibility of the adsorb layers, not only by their conformation.

## Effects of Applied Load and Contact Time on Intersurface Adhesion

To investigate the effects of compressive loading and time in contact on the adhesion between adsorbed QP2VP layers, we performed another experiment in which, after initial adsorption of QP2VP at pH 7.5 and the subsequent drop in pH to 3.9, the cell was flushed with pure water at natural pH, *i.e.*, pH 5.5. Presumably, any QP2VP that remains on the surface after flushing is, therefore, irreversibly adsorbed, at least on the time scale of these experiments. The resulting force

profile for this system is shown in Figure 4. The long-range interaction forces are similar in form to those obtained in the presence of electrolyte, over the range of solution pHs used. This is clearly illustrated when comparing the data in Figures 2 and 4. There is a long-range double layer interaction, a jump into contact at a small surface separation and short-range incompressible hard wall repulsion. The fact that there is hard wall repulsion clearly indicates that flushing the cell has not removed all of the adsorbed QP2VP. In fact, the hard wall is at a surface separation of 1.4 nm, which is comparable with that obtained prior to flushing (see Table 1). Additionally, the surface separation at which the jump into contact occurs is also within error of that obtained

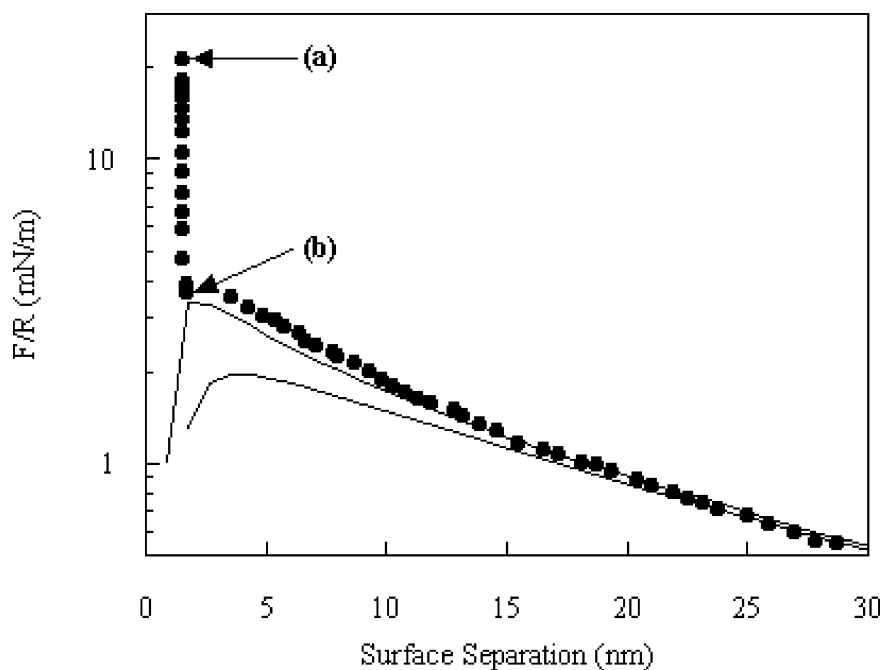


**FIGURE 4** Semilog plot of normalised force versus surface separation between mica surfaces with adsorbed QP2VP in Milli-Q water at natural pH and no added electrolyte. The solid curves represent the DLVO theoretical fit to the experimental data. The best fit was obtained using a Hamaker constant of  $2.2 \times 10^{-20}$  J,  $\psi_0 = 100$  mV, and a Debye length of 21 nm. The upper and lower limits are the constant charge and constant potential boundary conditions, respectively. At position (a), a surface separation of 1.4 nm, the surfaces are in contact under a small compressive load, while position (b) is at 1.8 nm and is the contact position under a zero compressive load.

at a similar pH prior to flushing (*i.e.*, pH 6.3; data are shown in Figure 3).

The one significant effect that flushing the cell has on the force profile is that it leads to an increase in range of the double layer repulsion. To highlight this, Figure 4 also contains the DLVO fit to the data, performed as detailed above, which yields a Debye length of 21 nm and a surface potential,  $\psi_0$ , of 100 mV. As expected, because the electrolyte concentration is low, the Debye length, and hence the range of the repulsion, is greater than that obtained in the presence of electrolyte (see Table 1). However, flushing the cell results in a drop in surface potential to 100 mV, as compared with  $\psi_0$  120 mV at pH 6.3 and 115 mV at pH 3.9 (Table 1) obtained prior to flushing. Again, this is an expected result since the surface potential is dominated by the charge on the polyelectrolyte, as discussed above. Hence, flushing the cell will remove some of the loosely surface-associated polyelectrolyte, thereby decreasing the net surface potential. Interestingly, this decrease in net potential is small, indicating that only a small amount of QP2VP is desorbed. This is consistent with the fact that there is no significant change in the position of the hard wall after flushing.

We measured adhesion as a function of time in contact and compressional load for the flushed system at natural pH. Specifically, the surfaces were allowed to remain in contact for a period of time ranging from one to ten minutes under a small positive loading (small compression of the layers) and a zero applied load, *i.e.*, the point at which the surfaces jump into contact, and there is no external compression of the adsorbed layers. The positions on the force profile corresponding to these two loads are denoted in Figure 4 as (a) and (b), respectively. Position (a) is at surface separation of 1.4 nm and each layer has been slightly compressed by 0.2 nm, while position (b) is at a surface separation of 1.8 nm. Note that the value of  $F/R$  corresponding to these two points is not the applied load but a measure of the electrosteric repulsive interaction (see above). Also note that, during decompression, the positions of the outward jumps were all from a surface separation of around 1.8 nm and there was no flattening of the surfaces.

The adhesion measured between the QP2VP layers when the surfaces were allowed to remain at position (b), *i.e.*, in contact under no positive loading, are shown in Table 3. This table presents the results for eight successive adhesion measurements, *i.e.*, compression/decompression cycles, presented in the sequential order in which the measurements were performed. Note that duplicate measurements of adhesion were made for each time, and the average of these is shown in Table 3. Also note that the surfaces were separated

**TABLE 3** Data Showing the Adhesions Measured on a Series of Compression/Decompression Cycles

Compression/decompression cycle	Time in contact (mins)	Force of adhesion ( $\text{mN}\cdot\text{m}^{-1}$ )
1	1	2.1
2	5	13.3
3	10	20.5
4	1	9.5

Specifically, the adsorbed QP2VP layers were brought into contact under zero compressive load and adhesion measured as a function of time in contact.

The numbering of the compression/decompression cycle represents the sequential order of the measurements.

for 4–5 min between each compression/decompression cycle. The adhesion between the layers was found to depend both on the time in contact and the compression history of the layers. Specifically, the magnitude of the force of adhesion increases with the time in contact. The results in Table 3 clearly indicate that the longer the surfaces are left in contact under zero applied load, the more time the adsorbed polyelectrolyte has to maximise adhesion since time is required to optimise both attractive segment-segment (chain entanglement) and segment-surface interactions (intersurface bridging). Both these bridging mechanisms proposed by Åkesson *et al.* [5] and Maurdev *et al.* [18] rely on conformational rearrangement of the adsorbed polyelectrolyte, and clearly these molecular rearrangements occur on a time scale comparable with that of each compression/decompression cycle.

Another interesting observation is that at zero applied load, the adhesion is affected by the number of compression/decompression cycles to which the system has been subjected (see Table 3). Specifically, the adhesion after 1 min in contact for compression/decompression 4 ( $9.5 \text{ mN m}^{-1}$ ) is greater than that obtained for the first compression/decompression cycle ( $2.1 \text{ mN m}^{-1}$ ), even though the time in contact and loading are the same. It is likely that after optimising adhesion during compression/decompression 3, by maintaining contact for 10 min, the adsorbed layers do not completely relax back to their unperturbed conformation: that is to say, the system has some memory of its prior compression history, at least on the time scale of each compression/decompression cycle.

Interestingly, when the surfaces are left in contact under a small compressional load, *i.e.*, position (a) in Figure 4, the amount of time in contact has no effect whatsoever on the intersurface adhesion,



even if contact is maintained for as long as 120 min. The adhesion repeatedly measured at this load irrespective of time in contact is approximately  $26 \text{ mN m}^{-1}$ . This is a comparatively large adhesion (see Table 3). In fact, when the applied load is zero, it is only after maintaining contact for 10 min that the adhesion is comparable with this, *i.e.*,  $20 \text{ mN m}^{-1}$ . It appears that the small compressive loading, which brings the surfaces closer together by 0.4 nm, facilitates polyelectrolyte bridging: it is easier for the polyelectrolyte chains to bridge across from one surface to another, and the process of chain entanglement can occur more rapidly. Thus, adhesion is maximised and the time required for this maximisation is reduced.

## CONCLUSIONS

We have shown that the adsorption and subsequent surface forces between QP2VP layers are strongly dependent on solution pH and compression of the layers. The interaction forces consist of a long-range repulsive double-layer interaction, shorter-range electrosteric forces, and attractive bridging forces that lead to intersurface adhesion. The positively charged QP2VP layer dominates the double-layer component of the repulsive interaction. The bridging attractive forces are due to both intersurface bridging and polyelectrolyte chain entanglement. These are extremely sensitive to the conformation of the adsorbed polyelectrolyte, which changes significantly with solution pH.

Surface forces measured on compression of the adsorbed QP2VP layer do not always clearly reflect changes in the adsorbed conformation and surface excess of the polyelectrolyte. However, the polyelectrolyte conformation is manifest more dramatically on measurement of the adhesion, upon retraction of the surfaces or decompression of the adsorbed layers. There is a strong dependence of the adhesion between the polyelectrolyte layers on the compressive load, time in contact, and compression history since the molecular rearrangements required for chain entanglement and intersurface bridging occur on a long time scale, *i.e.*, of the order of minutes. Under a small compressive load, the surfaces are closer together, facilitating segment-surface and segment-segment interactions across the two interacting layers.

## REFERENCES

- [1] Afshar-Rad, T., Bailey, A. I., Luckham, P. F., MacNaughtan, W., and Chapman, D., *Colloids Surf.* **25**, 263–277 (1987).

- [2] Marra, J., and Hair, M., *J. Phys. Chem.* **92**, 6044–6051 (1988).
- [3] Dahlgren, M. A. G., and Claesson, P. M., *Progr. Colloid Polym. Sci.* **93**, 206–208 (1993).
- [4] Dahlgren, M. A. G., Waltermo, Å., Blomberg, E., Claesson, P. M., Sjöström, L., Åkesson, T., and Jönsson, B., *J. Phys. Chem.* **97**, 11769–11775 (1993).
- [5] Åkesson, T., Woodward, C., and Jönsson, B., *J. Chem. Phys.* **91**, 2461–2469 (1989).
- [6] Woodward, C. E., Åkesson, T., and Jönsson, B., *J. Chem. Phys.* **101**, 2569–2576 (1994).
- [7] Pincus, P., *Macromolecules* **24**, 2912–2919 (1991).
- [8] Böhrer, M. R., Evers, O. A., and Scheutjens, J. M. H. M., *Macromolecules* **23**, 2288–2301 (1990).
- [9] Evers, O. A., Fleer, G. J., Scheutjens, J. M. H. M., and Lyklema, J., *J. Colloid Interface Sci.* **111**, 446–454 (1986).
- [10] Dahlgren, M. A. G., Claesson, P. M., and Audebert, R., *J. Colloid Interface Sci.* **166**, 343–349 (1994).
- [11] Bremmell, K. E., Jameson, G. J., and Biggs, S., *Colloids Surf. A* **139**, 199–211 (1998).
- [12] Claesson, P. M., Dahlgren, M. A. G., and Eriksson, L., *Colloids Surf. A* **93**, 293–303 (1994).
- [13] Claesson, P. M., Paulson, O. E. H., Blomberg, E., and Burns, N. L., *Colloids Surfs. A* **123–124**, 341–353 (1997).
- [14] Dahlgren, M. A. G., *Langmuir* **10**, 1580–1583 (1994).
- [15] Dahlgren, M. A. G., Hollenberg, H. C. M., and Claesson, P. M., *Langmuir* **11**, 4480–4485 (1995).
- [16] Maurdev, G., *PhD Thesis*, University of Melbourne, Australia (2001).
- [17] Fleer, G. J., Cohen Stuart, M. A., Scheutjens, J. M. H. M., Cosgrove, T., and Vincent, B., *Polymers at Interfaces* (Chapman and Hall, New York, 1994).
- [18] Maurdev, G., Meagher, L., Ennis, J., and Gee, M. L., *Macromolecules* **34**, 4151–4158 (2000).
- [19] Neivandt, D. J., and Gee, M. L., *Langmuir* **11**, 1291–1296 (1995).
- [20] Weast, R. C., *Handbook of Chemistry and Physics*, 64th ed. (CRC Press, Boca Raton FL) pp. 1983–1984.
- [21] Israelachvili, J. N., and Adams, G. E., *J. Chem. Soc. Faraday Trans. 1*, **74**, 975–1001 (1978).
- [22] Horn, R. G., and Smith, D. T., *Appl. Opt.*, **30**, 59–65 (1991).
- [23] Israelachvili, J. N., *Intermolecular and Surface Forces*, 2nd ed. (Academic Press, New York, 1992).
- [24] Stewart, A. M., and Christenson, H. K., *Meas. Sci. Technol.* **1**, 1301–1303 (1990).
- [25] Stewart, A., *J. Colloid Interface Sci.* **170**, 287–289 (1995).
- [26] Hunter, R. J., *Foundations of Colloid Science*, Vol. 1 (Clarendon, Oxford, 1987).
- [27] McCormack, D., Carnie, S. L., and Chan, D. Y. C., *J. Colloid Interface Sci.* **169**, 177–196 (1995).
- [28] Pashley, R. M., *J. Colloid Interface Sci.* **80**, 153–162 (1981).
- [29] Pashley, R. M., *J. Colloid Interface Sci.* **83**, 531–546 (1981).
- [30] Pashley, R. M., and Quirk, J. P., *Colloids Surf.* **9**, 1–17 (1984).